

Article

# Uraninite, Coffinite and Brannerite from Shear-Zone Hosted Uranium Deposits of the Bohemian Massif (Central European Variscan Belt)

Miloš René <sup>1,\*</sup> and Zdeněk Dolníček <sup>2</sup>

<sup>1</sup> Institute of Rock Structure and Mechanics, v.v.i., Academy of Sciences of the Czech Republic, V Holešovičkách 41, Prague 8, 182 09, Czech Republic

<sup>2</sup> Department of Geology, Palacký University, 17. listopadu 12, Olomouc 771 46, Czech Republic; dolnicek@prfnw.upol.cz

\* Correspondence: rene@irsm.cas.cz; Tel.: +420-266-009-228

Academic Editor: Mostafa Fayek

Received: 31 January 2017; Accepted: 22 March 2017; Published: 29 March 2017

**Abstract:** New mineralogical data are presented for shear-zone hosted uranium mineralisation from selected uranium deposits that occur in the Bohemian Massif. The uranium mineralisation is in high-grade metamorphic rocks of the Moldanubian Zone and/or in granitic rocks of the Moldanubian batholith and Bor pluton as complex uraninite–coffinite and uraninite–coffinite–brannerite assemblages. For analysed coffinites and brannerites, anomalous enrichment of Y (up to 3.4 wt %  $Y_2O_3$ ) and Zr (up to 13.8 wt %  $ZrO_2$ ) is significant. The microprobe data indicate that coffinites from the Rožná and Okrouhlá Radouň uranium deposits contain variable PbO (0–4.3 wt %), FeO (0–2.5 wt %),  $Al_2O_3$  (0–3.5 wt %),  $P_2O_5$  (0–1.8 wt %), and CaO (0.7–3.5 wt %). Brannerite is present in unaltered and altered grains with variable concentrations of  $U^{4+}$  (0–0.5 apfu),  $U^{6+}$  (0.06–0.49 apfu), Ti (0.90–2.63 apfu), Ca (0.09–0.41 apfu), and low concentrations of Al (0–0.19 apfu), Th (0–0.04 apfu), Y (0–0.08 apfu), Zr (0–0.13 apfu) and REE (0–0.14 apfu).

**Keywords:** uranium; hydrothermal mineralisation; granite; high-grade metamorphic rocks; aceite; Bohemian Massif; Rožná; Okrouhlá Radouň; Zadní Chodov; Lhota

## 1. Introduction

The Bohemian Massif is part of the European Variscan belt, which hosts a significant quantity of uranium deposits bound by brittle shear zones developed in high-grade metamorphic rocks and/or granites [1–4]. According to [5], these deposits are classified as metamorphic deposits (e.g., Beaverlodge district and Fay-Verna deposits, Canada) and/or vein deposits without any relation to granitic intrusions (e.g., Schwarzwald, USA). In the Bohemian Massif, this group of uranium deposits is represented by the Rožná and Okrouhlá Radouň ore deposits in the high-grade metamorphic rocks of the Moldanubian Zone [3,6] and by the Zadní Chodov, Vítkov II, and Lhota ore deposits in the area of the Bor pluton [7]. Apart from the predominant vein-type deposits in the Krušné Hory/Erzgebirge Mts. (Schlema-Alberoda, Jáchymov) and the Příbram uranium deposits, these deposits show no direct genetic relationship between mineralisation and granitic plutons (Figure 1).

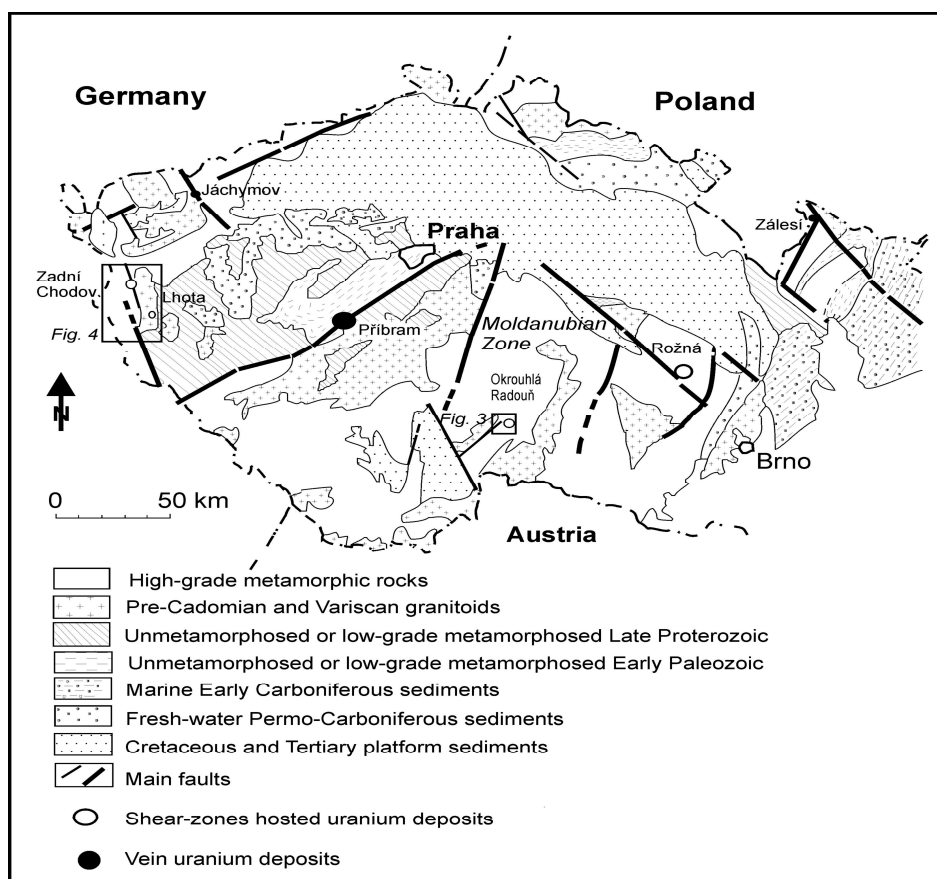


**Figure 1.** Simplified geological map of the Bohemian Massif with the most significant hydrothermal uranium deposits.

The subconformity epimetamorphic deposits consist of peneconcordant lenses or highly disseminated uranium mineralisation evolved in fractures and/or brecciated shear zones. The host rocks (high-grade metamorphic and/or granitic rocks) of these deposits are strongly altered, exhibiting extensive albitisation, chloritisation, and hematitisation. These metasomatic rocks, consisting mostly of albite and chlorite with subordinate hematite and carbonate, are named aceites according to the recent International Union of Geological Sciences (IUGS) classification. Aceites are defined as low-temperature alkaline metasomatic rocks, which are closely associated with uranium mineralisation [8].

According to their mineral composition, the aceites are very similar to episyenites developed in uranium deposits of the Massif Central and the Armorican massif in France, linked with leucogranite plutons. Episyenites are defined as igneous-like rocks of syenite composition, displaying cavities produced by hydrothermal dissolution of quartz grains that can ultimately host uranium ore deposits [9]. Both rock types are products of low-temperature alkaline metasomatism associated with a significant input of  $\text{Na}_2\text{O}$  and the loss of  $\text{SiO}_2$ . The parent hydrothermal solutions are usually oxidized and enriched in Na. Distinctly different mineral compositions have metasomatic deposits, which originated by high-temperature alkali metasomatism (e.g., Central Ukraine). Metasomatic facies in these uranium deposits include albitites, aegirinites, and alkali-amphibole rich rocks [5]. In the recent IUGS classification of metamorphic rocks, these metasomatic rocks are classified as fault-related metasomatites, which are common in Precambrian shields [8].

The aceite-hosted uranium deposits in the Bohemian Massif display anomalous rare earth elements (REE), Y, and Zr mobility associated with uranium mineralisation [2,4]. The objectives of this paper are to present the detailed mineralogy of uranium minerals (uraninite, coffinite, brannerite), as

well as to assess the behaviour of Y and Zr during the hydrothermal alteration processes in uranium ore deposits that occur (i) in high-grade metamorphic rocks of the Moldanubian Zone (Rožná, Okrouhlá Radouň); (ii) at the boundary between high-grade metamorphic rocks of the Moldanubian Zone and granitic rocks of the Moldanubian plutonic complex (Okrouhlá Radouň) and (iii) within the Bor granite pluton (Zadní Chodov, Lhota). For these uranium deposits, a low-temperature metasomatism is significant, associated with infiltration of oxidized basinal fluids into the crystalline rocks of the Moldanubian Zone. The wide range of salinities of fluids is interpreted as a result of the large-scale mixing of basinal brines with meteoric water [3].

## 2. Geological Setting

### 2.1. Rožná Uranium Deposit

The Rožná uranium deposit lies in the NE part of the Moldanubian Zone. The high-grade metamorphic rocks of this zone were overthrust on the NE boundary by the Svatka Crystalline Unit and by the Cadomian Brunovistulian foreland. The host rocks of this uranium deposit consist mainly of biotite paragneisses and amphibolites with small bodies of calc-silicate rocks, marbles, serpentinites, and pyroxenites. Longitudinal N–S to NNW–SSE striking ductile shear zones (Rožná and Olší shear zones) dip WSW at an angle of 70°–90° and strike parallel to the tectonic contact between the Gföhl unit of the Moldanubian Zone and the Svatka Crystalline Unit.

The main longitudinal faults of the Rožná shear zone are designated as Rožná 1 (R1) and Rožná 4 (R4) and host the main part of the disseminated uranium mineralisation. The less strongly mineralised Rožná 2 (R2) and Rožná 3 (R3) fault zones host numerous separate pinnate carbonate veins (Figure 2). Longitudinal fault structures are crosscut and segmented by ductile to brittle NW–SE and SW–NE-striking fault zones that host post-uranium carbonate-quartz-sulphide mineralisation.

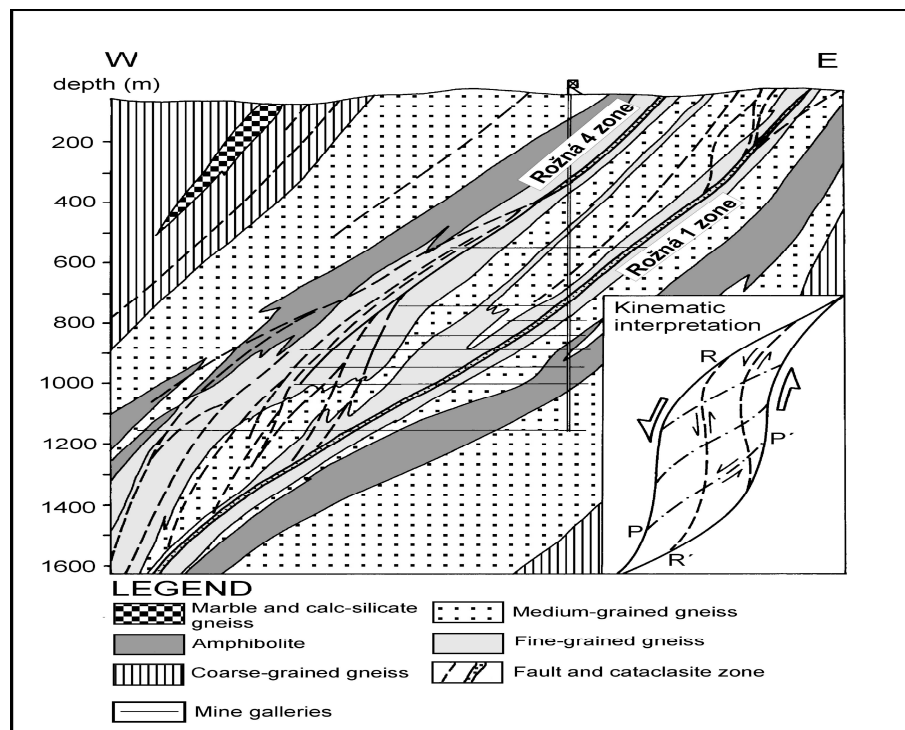


Figure 2. Schematic cross section of the Rožná uranium deposit, modified from [4].

Uranium mineralisation forms (i) disseminated coffinite > uraninite > brannerite in chloritised, pyritised, carbonatised, and graphite-enriched cataclastites of longitudinal faults; (ii) uraninite >

coffinite in carbonate veins; (iii) disseminated coffinite > uraninite in desilicified, albitized, and hematitized rocks (aceites) adjacent to longitudinal faults and (iv) mostly coffinite bound to the intersection of fault zones with diagonal and longitudinal structures.

Total mine production of the Rožná uranium deposit was 17,241 t U with an average ore grade of 0.24% U, mined from 1957 to 2000 [10]. The Rožná uranium deposit is the last recently mined uranium deposit in Central Europe with an annual production of about 300 t U.

## 2.2. Okrouhlá Radouň Uranium Deposit

The Okrouhlá Radouň uranium deposit is situated in a NNW–SSE striking shear zone on the north-eastern margin of the Klenov pluton, which is a part of the Moldanubian plutonic complex (Figure 1). The host-rock series comprises migmatized high-grade metasediments of the Moldanubian Zone and two-mica leucogranites of the Klenov pluton (Figure 3). Granites that formed a series of the NE–SW to NNE–SSW-elongated sheets or larger irregular bodies with sheeted margins intruded into the high-grade metasediments. The sheets are mostly parallel to the foliation in the metasediments. The Klenov pluton was emplaced during the Variscan magmatic event (327 Ma, U/Pb analyses of monazite) in a deeper part of the exhumed high-grade metamorphic rocks ( $P = 0.35$  GPa,  $T = 500$ – $600$  °C) closely related to the development of the mid- to upper-crustal NNE–SSW metamorphic fabrics [11].

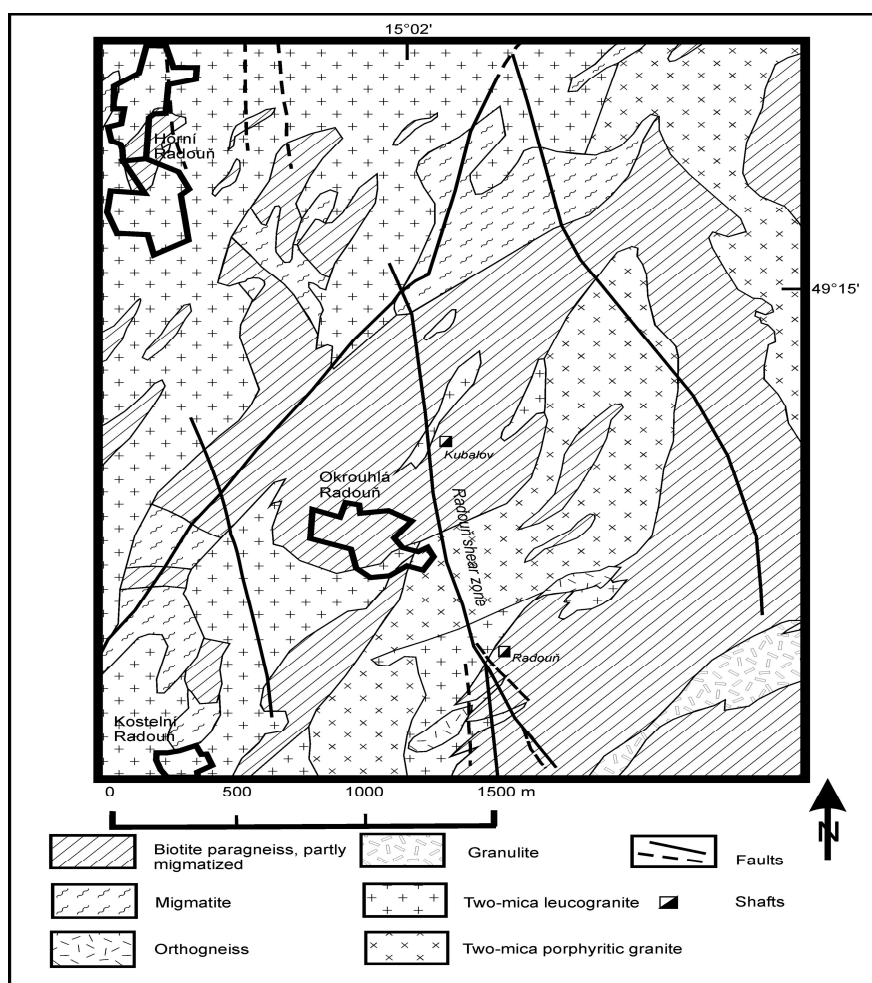


Figure 3. Geological setting of the Okrouhlá Radouň uranium deposit (modified from [6]).

The most significant mineralised structure in this area, the Radouň shear zone (86.6% of total mined U), was explored along a strike length of approximately 3 km and to a depth of 650 m (Figure 3). The highest-grade uranium mineralisation was developed at depths of 250–400 m beneath the present surface. The thickness of the mineralised zone is highly variable, ranging from 30 cm to approximately 7 m. The thickest portion of this zone was observed in the southern part of the uranium deposit, where a shear zone was developed in altered two-mica leucogranites and in highly hydrothermally altered, partly migmatised biotite paragneisses. The shear zone is in-filled with cataclasites formed by host-rock breccia, which were altered to clay-mineral-rich and chlorite-rich assemblages containing a disseminated uranium mineralisation comprising mainly coffinite and lesser amounts of uraninite.

The Okrouhlá Radouň uranium deposit was mined from 1972 to 1990 and belongs among smaller uranium deposits in the Bohemian Massif. The total mine production of low-grade uranium ore (0.084 wt % U) was 1300 t U [10].

### 2.3. Zadní Chodov Uranium Deposit

The Zadní Chodov uranium deposit, which is located in the northern tectonic block of the Bor pluton, was developed by mine workings down to a level of 1250 m with a length of over 2.5 km. Uranium mineralisation is associated with the N–S trending zones of the Zadní Chodov fault in areas of their intersection with NW–SE trending fault structures, which represent a NW continuation of the Central fault (Figure 4). The infill of the shear zones consists of intensely altered and crushed rocks with chlorite-rich and/or clay-mineral-rich assemblages. Uranium mineralisation was concentrated into three shear zones (CH-1, CH-4, and CH-11). The thickness of individual shear zones is highly variable from 30 cm to approximately 1–2.5 m. The total thickness of these mineralised shear zones is 50–150 m. The high-grade uranium mineralisation was developed at depths of 440–960 m beneath the present surface. The most common uranium minerals are coffinite (65 vol %), uraninite (25 vol %) and brannerite (10 vol %). The U/Pb age of brannerite is  $185 \pm 6$  Ma (thermal ionization mass spectrometry, ID–TIMS) and is interpreted to reflect the Mesozoic recrystallisation of original Variscan brannerite [12].

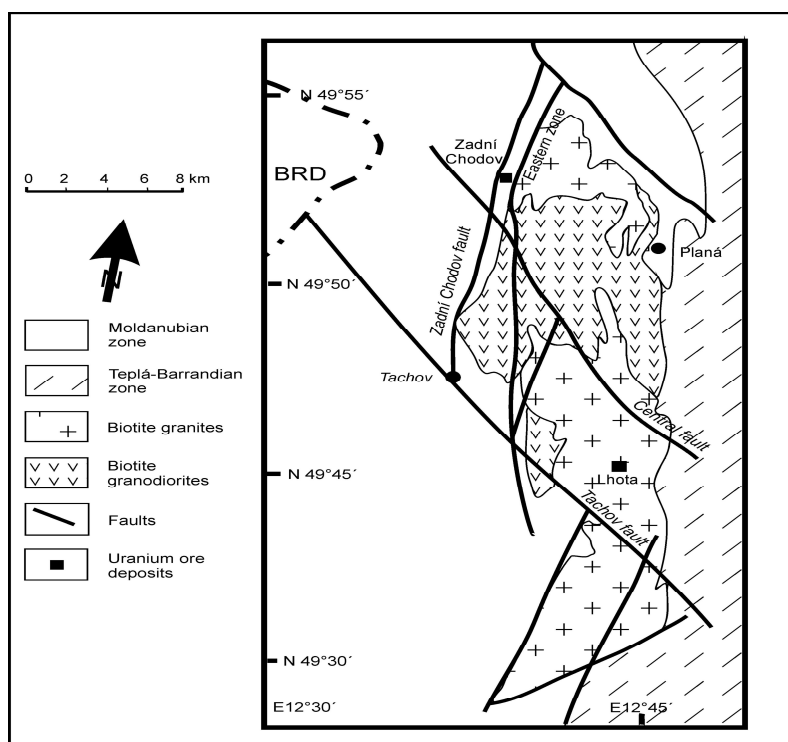


Figure 4. Geological map of the Bor pluton, modified from [7].

The Zadní Chodov uranium deposit was mined from 1952 to 1992 and was ranked among medium-size uranium deposits in the Bohemian Massif. The total mine production of low-grade uranium ore (0.195 wt % U) was 4151 t U [10].

#### 2.4. Lhota Uranium Deposit

The small uranium deposit Lhota is situated in the central block of the Bor pluton. In comparison with the other shear-zone hosted uranium deposits in the Bohemian Massif (Rožná, Okrouhlá Radouň) where coffinite and uraninite predominate, in the uranium mineralisation developed in the Bor pluton and surrounding high-grade metamorphic rocks, brannerite is another significant uranium ore mineral.

The most voluminous rocks in the Bor pluton are usually coarse-grained porphyritic biotite granites. These granites intruded during the Variscan magmatic event ( $337 \pm 6$  Ma, U/Pb TIMS analyses on zircon; [13]). In the northern block of the Bor pluton, older amphibole-biotite granodiorites, tonalites, and quartz diorites were also observed (Figure 4).

The area surrounding this uranium deposit consists of mostly coarse-grained biotite granites together with smaller bodies of amphibole-biotite granodiorites and tonalites overlain by remnants of the Moldanubian metamorphic rocks. The two ore-bearing shear structures (Os-2, Os-17) strike NW-SE and dip steeply NE. The thickness of these mineralised shear zones ranges from 5 to 18 m. The uranium mineralisation comprises coffinite, uraninite, and brannerite. The U/Pb age of uraninite II from the post-ore quartz stage is  $158 \pm 3$  Ma (ID-TIMS) [12].

The Lhota uranium deposit was explored between 1953–1967 and 1975–1989 by five exploration shafts down to a depth of 250 m, and by numerous boreholes down to levels of 300 m to 600 m. During these two exploration stages, low-grade uranium mineralisation (0.120 wt % U) of 158 t U [10] was found, but not mined.

### 3. Material and Methods

Representative samples of ore mineralisation from all the above mentioned uranium deposits were collected during exploration and mining of the Czechoslovak Uranium Industry enterprise (recently DIAMO). A majority of samples from the Rožná deposit originated from a deeper part of the main shear zone (R1). The fault zone R1 comprises massive cataclasite that is 4–15 m thick, traceable over the horizontal distance of 15 km. The zones strike  $340^\circ$ – $355^\circ$  and dip west at an angle of  $45^\circ$ – $70^\circ$ . The ore is composed of uraninite, coffinite, and brannerite disseminated in chloritised, hematitised, argillitised, and pyritised coherent and incoherent cataclasites and fault breccias. Ore lenses are 3.5 m thick on average. The grade is around 0.5 wt % U on average, and up to 10 wt % U locally [3].

The samples of uranium mineralisation from the Okrouhlá Radouň deposit were taken in the thickest, southern part of the Radouň shear zone (OR-3b). In this place the thickness of the mineralised zone was about 7 m and this fault cut altered two-mica leucogranites and partly migmatised biotite paragneisses. Mylonitised host rocks, partly altered to kaolinite, smectite, and chlorite, fill up the fault cuts. The ore bodies are associated with intensely altered metamorphic and granitic rocks containing significant amounts of albite, calcite, and hematite [6].

Samples from the Zadní Chodov deposit, enriched in brannerite, were collected in the deepest part of the main ore zone (CH-1). The thickness of this shear zone is highly variable from 30 cm to approximately 1–2.5 m. The infill of the CH-1 shear zone consists of intensely altered and crushed partly migmatised biotite paragneisses with chlorite-rich and/or clay mineral-rich (illite, kaolinite) assemblages with local accumulations of carbonaceous matter [7].

Samples with coffinite were collected from an exploration borehole in the area of the Lhota deposit (ore zone Os-2). This main ore-bearing shear structure strikes NW-SE and dips steeply NE. The thickness of the mineralised zone is 5–18 m. The infill of the Os-2 shear zone consists of intensely crushed and altered biotite granites of the Bor pluton with chlorite- and albite-rich assemblages [7].

The uranium minerals were analysed in polished thin sections. Back-scattered electron (BSE) images were acquired to study the internal structure of mineral aggregates and individual mineral

grains. The abundances of Al, As, Bi, Ca, Ce, Dy, Er, Eu, F, Fe, Gd, Hf, Ho, La, Lu, Mg, Mn, Nb, Nd, P, Pr, Sc, Si, Sm, Th, U, W, Y, Yb, and Zr were determined using a CAMECA SX-100 electron microprobe (CAMECA SAS, Gennevilliers Cedex, France) operated in wavelength-dispersive-Xray (WDX) mode at the Institute of Geological Sciences, Masaryk University in Brno. The accelerating voltage and beam currents were 15 kV and 20 nA or 40 nA, respectively, and the beam diameter was 1  $\mu\text{m}$  to 5  $\mu\text{m}$ . The peak count time was 20 s, and the background time was 10 s for major elements. For the trace elements, the times were 40–60 s on the peaks, and 20–30 s on the background positions. The raw data were corrected using peak-to-average power (PAP) matrix corrections [14]. The detection limits were approximately 400–500 ppm for Y, 600 ppm for Zr, 500–800 ppm for REE, and 600–700 ppm for U and Th.

#### 4. Mineralogy

The predominant uranium mineral in the samples from all of the studied uranium deposits was coffinite. Uraninite, which was also identified in our samples from the Rožná and Okrouhlá Radouň ore deposits, is relatively rare. The brannerite was identified in uranium mineralisation from the Rožná and Zadní Chodov deposits. However, brannerite is a highly significant uranium mineral for the deeper parts of the Zadní Chodov uranium deposit.

##### 4.1. Uraninite

Uraninite from the Okrouhlá Radouň uranium deposit occurs usually as small colloform aggregates that are overgrown by coffinite and/or is observed as relics enclosed in highly heterogeneous aggregates of coffinite (Figure 5A,B). Both uranium minerals from the Rožná and Okrouhlá Radouň deposits commonly form rims around chlorite flakes and pyrite grains (Figure 6A,B). The  $\text{SiO}_2$  and  $\text{UO}_2$  contents in uraninite from Rožná vary from  $\text{UO}_{2+x}$  to  $\text{USiO}_4$ , indicating that highly variable coffinitisation of uraninite occurred in the main shear zones of this uranium deposit (Figure 7). Almost all uraninite aggregates were replaced by coffinite to a variable degree, as is demonstrated by the high  $\text{SiO}_2$  contents (6.3–13.0 wt %). In addition, the microprobe data revealed variable  $\text{PbO}$  (0–1.5 wt %),  $\text{FeO}$  (0.2–0.9 wt %),  $\text{Al}_2\text{O}_3$  (0.6–1.7 wt %),  $\text{P}_2\text{O}_5$  (0–0.2 wt %), and  $\text{CaO}$  (2.5–3.9 wt %) contents in the examined uraninite (Table 1).

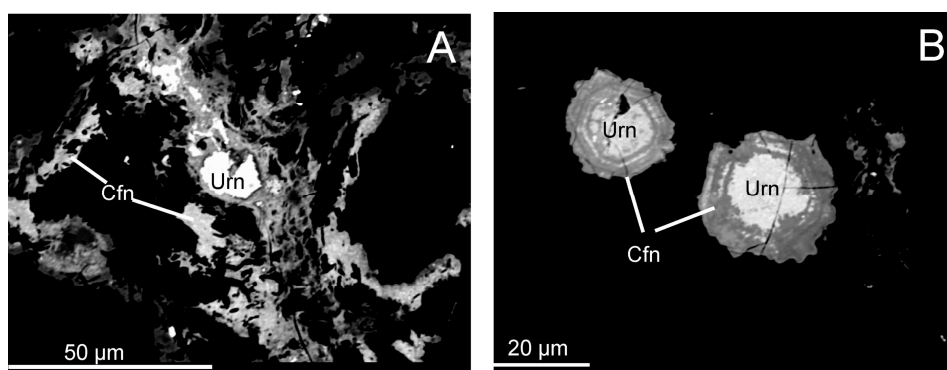


**Figure 5.** Back-scattered electron (BSE) images of the uranium mineralisation taken by P. Gadas and R. Škoda: (A) Heterogeneous aggregates of coffinite (Cfn), partly originated by coffinitisation of uraninite (Urn), Okrouhlá Radouň; (B) Overgrowth of coffinite (Cfn) on uraninite (Urn), Okrouhlá Radouň.

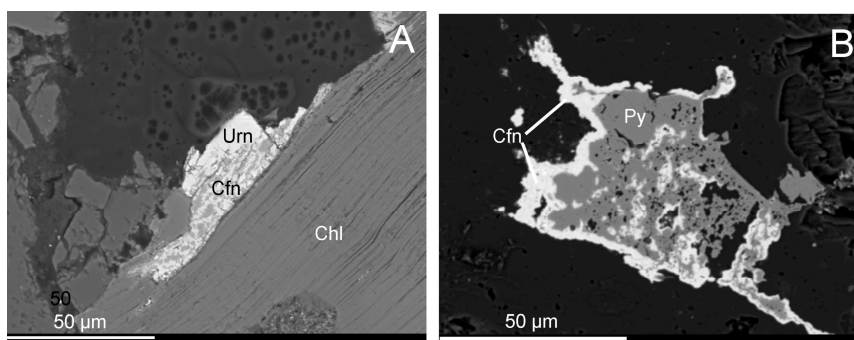


**Figure 6.** BSE images of the uranium mineralisation taken by P. Gadas and R. Škoda: (A) Rims of uraninite (Urn) and coffinite (Cfn) around chlorite flakes (Chl), Rožná; (B) Coffinite (Cfn) rims around pyrite grains (Py), Okrouhlá Radouň.

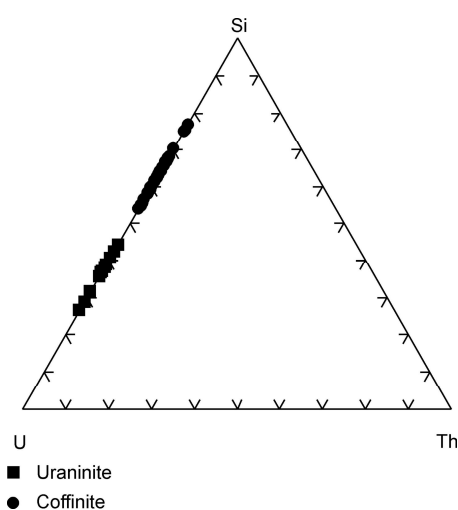


**Figure 7.** Chemical composition of coffinite and uraninite from Rožná (wt %).

**Table 1.** Representative WDX analyses of uraninite.

Sample	1-1	1-5	1-9	1-10	02-6	02-7	02-11	02-14
Locality (wt %)	Rožná	Rožná	Rožná	Rožná	Okrouhlá Radouň	Okrouhlá Radouň	Okrouhlá Radouň	Okrouhlá Radouň
SiO <sub>2</sub>	7.05	10.19	9.45	12.41	2.29	2.19	2.07	2.61
P <sub>2</sub> O <sub>5</sub>	0.13	0.00	0.00	0.09	0.12	0.08	0.11	0.05
Al <sub>2</sub> O <sub>3</sub>	0.64	1.02	0.89	1.12	0.05	0.08	0.07	0.09
ZrO <sub>2</sub>	0.41	b.d.l.	b.d.l.	0.17	0.00	b.d.l.	b.d.l.	b.d.l.
TiO <sub>2</sub>	0.10	0.30	0.01	0.10	n.d.	n.d.	n.d.	n.d.
CaO	3.42	2.98	3.88	3.13	3.26	3.36	3.50	3.30
FeO	0.70	0.85	0.35	0.34	0.85	0.92	0.73	0.76
MnO	n.d.	n.d.	n.d.	n.d.	0.25	0.66	0.21	0.39
Sc <sub>2</sub> O <sub>3</sub>	n.d.	n.d.	n.d.	n.d.	b.d.l.	b.d.l.	0.08	0.02
As <sub>2</sub> O <sub>5</sub>	n.d.	n.d.	n.d.	n.d.	0.46	0.32	0.39	0.40
Y <sub>2</sub> O <sub>3</sub>	0.11	0.03	0.26	0.35	0.33	0.23	0.17	0.24
La <sub>2</sub> O <sub>3</sub>	0.04	0.14	0.23	0.18	b.d.l.	b.d.l.	b.d.l.	b.d.l.
Ce <sub>2</sub> O <sub>3</sub>	0.14	0.21	0.44	0.34	0.00	0.04	b.d.l.	b.d.l.
Pr <sub>2</sub> O <sub>3</sub>	n.d.	n.d.	n.d.	n.d.	0.04	0.01	0.10	0.02
Nd <sub>2</sub> O <sub>3</sub>	n.d.	n.d.	n.d.	n.d.	0.03	b.d.l.	0.08	b.d.l.
Gd <sub>2</sub> O <sub>3</sub>	n.d.	n.d.	n.d.	n.d.	0.09	0.02	b.d.l.	0.07
Dy <sub>2</sub> O <sub>3</sub>	n.d.	n.d.	n.d.	n.d.	0.05	0.19	0.04	0.09
Er <sub>2</sub> O <sub>3</sub>	n.d.	n.d.	n.d.	n.d.	0.01	0.02	b.d.l.	0.01

Table 1. Cont.

Sample	1-1	1-5	1-9	1-10	02-6	02-7	02-11	02-14
Locality (wt %)	Rožná	Rožná	Rožná	Rožná	Okrouhlá Radouň	Okrouhlá Radouň	Okrouhlá Radouň	Okrouhlá Radouň
UO <sub>2</sub>	78.86	77.45	76.54	74.62	87.56	87.84	87.92	87.55
ThO <sub>2</sub>	b.d.l.	b.d.l.	b.d.l.	b.d.l.	b.d.l.	b.d.l.	b.d.l.	b.d.l.
PbO	1.39	0.22	0.57	0.09	2.99	2.71	3.12	3.06
Total	92.99	93.39	92.62	92.94	98.38	98.67	98.59	98.66
apfu, O = 4								
Si	0.50	0.67	0.63	0.77	0.18	0.18	0.17	0.21
P	0.01	0.00	0.00	0.01	0.01	0.01	0.01	0.00
Al	0.05	0.08	0.07	0.05	0.01	0.01	0.01	0.01
Zr	0.01	0.00	0.00	0.01	0.00	0.00	0.00	0.00
Ti	0.01	0.02	0.00	0.01	n.d.	n.d.	n.d.	n.d.
Ca	0.26	0.21	0.28	0.26	0.28	0.29	0.30	0.28
Fe	0.04	0.05	0.02	0.04	0.06	0.06	0.05	0.05
Mn	n.d.	n.d.	n.d.	n.d.	0.02	0.05	0.01	0.03
As	n.d.	n.d.	n.d.	n.d.	0.02	0.01	0.02	0.02
Y	0.00	0.00	0.01	0.01	0.01	0.01	0.01	0.01
La	0.00	0.01	0.01	0.00	0.00	0.00	0.00	0.00
Ce	0.01	0.01	0.01	0.01	0.00	0.00	0.00	0.00
Pr	n.d.	n.d.	n.d.	n.d.	0.00	0.00	0.00	0.00
Nd	n.d.	n.d.	n.d.	n.d.	0.00	0.00	0.00	0.00
Sm	n.d.	n.d.	n.d.	n.d.	0.00	0.00	0.00	0.00
Gd	n.d.	n.d.	n.d.	n.d.	0.00	0.00	0.00	0.00
Dy	n.d.	n.d.	n.d.	n.d.	0.00	0.01	0.00	0.00
Er	n.d.	n.d.	n.d.	n.d.	0.00	0.00	0.00	0.00
U	1.25	1.13	1.14	1.03	1.56	1.56	1.57	1.54
Th	0.00	0.00	0.00	0.00	0.00	0.00	0.00	0.00
Pb	0.03	0.00	0.01	0.00	0.06	0.06	0.07	0.07
Total	2.17	2.18	2.18	2.20	2.21	2.25	2.22	2.22

n.d.—not determined; b.d.l.—below detection limit.

The SiO<sub>2</sub> and UO<sub>2</sub> contents in uraninite from the Okrouhlá Radouň ore deposit vary in compositions near UO<sub>2+x</sub>. In addition, the analysed uraninite contains variable PbO (0–3.1 wt %), FeO (0.2–2.5 wt %), Al<sub>2</sub>O<sub>3</sub> (0–3.4 wt %), P<sub>2</sub>O<sub>5</sub> (0–1.8 wt %), and CaO (0.7–3.5 wt %) contents (Table 1).

#### 4.2. Coffinite

The coffinite occurs as distinctly heterogeneous aggregates (Figure 5A) and/or rims around chlorite flakes and pyrite grains (Figure 6A,B). The Zr-rich coffinite from the Okrouhlá Radouň uranium deposit was observed in the rim of altered zircon (Figure 8A). The coffinite occurring in shear zones at the Rožná ore deposit is commonly intimately associated with flakes of newly originated hydrothermal chlorite (Figure 8B). The SiO<sub>2</sub> and UO<sub>2</sub> contents in coffinite from the Rožná and Okrouhlá Radouň uranium deposits are close to stoichiometric USiO<sub>4</sub> (Figures 7 and 9). A majority of analysed coffinites from the Rožná and Okrouhlá Radouň ore deposits are enriched in Y<sub>2</sub>O<sub>3</sub> (up to 3.4 wt %) and ZrO<sub>2</sub> (up to 13.8 wt %; Table 2). The microprobe data further revealed variable PbO (0–4.3 wt %), FeO (0–2.5 wt %), Al<sub>2</sub>O<sub>3</sub> (0.8–3.5 wt %), P<sub>2</sub>O<sub>5</sub> (0–1.8 wt %), and CaO (0.7–3.5 wt %) contents in coffinites from the Rožná and Okrouhlá Radouň uranium deposits.

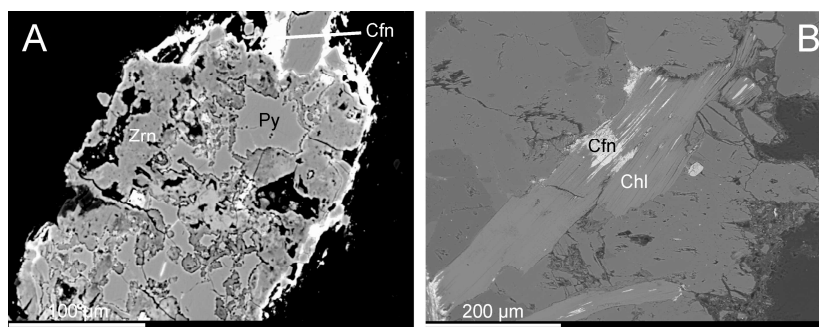


**Figure 8.** BSE images of the uranium mineralisation taken by P. Gadas and R. Škoda: (A) Highly altered zircon (Zrn) corroded by pyrite (Py) and rimmed by Zr-rich coffinite (Cfn), Okrouhlá Radouň; (B) Intimately associated coffinite (Cfn) with flakes of newly originated hydrothermal chlorite (Chl), Rožná.

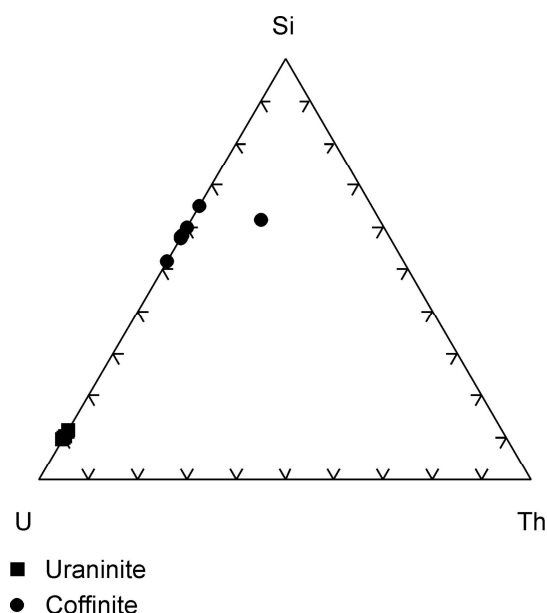


**Figure 9.** Chemical composition of coffinite and uraninite from the Okrouhlá Radouň (wt %).

**Table 2.** Representative WDX analyses of coffinite.

Sample	R-21-1	R-21-2	R-21-3	R-21-5	R-21-6	R-21-9	02-12	02-13	503-18	71-32	8036-4
Locality (wt %)	Rožná	Rožná	Rožná	Rožná	Rožná	Rožná	Okrouhlá Radouň				
SiO <sub>2</sub>	19.53	21.19	23.79	23.49	21.32	23.16	17.42	22.06	20.21	20.04	20.71
P <sub>2</sub> O <sub>5</sub>	0.14	0.12	b.d.l.	0.09	0.13	0.08	0.15	0.25	0.63	1.12	0.91
Al <sub>2</sub> O <sub>3</sub>	1.86	1.80	2.16	1.71	2.46	3.02	1.81	2.29	1.56	1.43	1.59
TiO <sub>2</sub>	1.46	1.20	0.94	0.89	1.50	1.35	n.d.	n.d.	n.d.	n.d.	n.d.
ZrO <sub>2</sub>	1.72	0.48	1.62	1.69	2.82	6.07	0.35	0.94	b.d.l.	1.08	0.00
CaO	2.56	2.21	2.43	1.87	3.00	2.71	1.62	2.28	3.28	3.01	1.62
FeO	1.53	0.30	b.d.l.	0.13	0.13	1.68	0.53	0.27	0.49	1.65	0.41
MnO	n.d.	n.d.	n.d.	n.d.	n.d.	n.d.	0.07	0.02	0.08	b.d.l.	0.05
Sc <sub>2</sub> O <sub>3</sub>	n.d.	n.d.	n.d.	n.d.	n.d.	n.d.	0.08	0.08	0.06	0.15	0.16
Y <sub>2</sub> O <sub>3</sub>	2.07	2.41	2.59	1.97	2.99	4.02	0.14	0.05	1.30	0.17	1.92
La <sub>2</sub> O <sub>3</sub>	n.d.	n.d.	n.d.	n.d.	n.d.	n.d.	0.07	0.13	b.d.l.	0.24	0.15
Ce <sub>2</sub> O <sub>3</sub>	1.67	2.05	2.34	1.72	2.98	2.21	0.45	0.58	b.d.l.	1.10	1.14
Pr <sub>2</sub> O <sub>3</sub>	n.d.	n.d.	n.d.	n.d.	n.d.	n.d.	b.d.l.	0.02	b.d.l.	0.15	0.17
Nd <sub>2</sub> O <sub>3</sub>	n.d.	n.d.	0.72	n.d.	n.d.	n.d.	0.11	0.02	b.d.l.	0.42	0.70
Sm <sub>2</sub> O <sub>3</sub>	n.d.	n.d.	n.d.	n.d.	n.d.	n.d.	b.d.l.	b.d.l.	b.d.l.	0.11	0.19
Gd <sub>2</sub> O <sub>3</sub>	0.44	0.40	n.d.	0.29	0.53	0.51	0.05	0.01	b.d.l.	0.25	0.34

Table 2. Cont.

Sample	R-21-1	R-21-2	R-21-3	R-21-5	R-21-6	R-21-9	02-12	02-13	503-18	71-32	8036-4
Locality (wt %)	Rožná	Rožná	Rožná	Rožná	Rožná	Rožná	Okrouhlá Radouň				
Dy <sub>2</sub> O <sub>3</sub>	n.d.	n.d.	n.d.	n.d.	n.d.	n.d.	b.d.l.	b.d.l.	b.d.l.	0.22	0.26
Er <sub>2</sub> O <sub>3</sub>	n.d.	n.d.	n.d.	n.d.	n.d.	n.d.	b.d.l.	0.01	b.d.l.	0.14	0.13
Yb <sub>2</sub> O <sub>3</sub>	0.18	0.01	b.d.l.	0.07	0.15	0.21	b.d.l.	b.d.l.	0.09	0.17	0.00
UO <sub>2</sub>	60.44	62.42	51.97	61.60	54.70	47.84	71.79	69.00	67.00	60.04	66.97
ThO <sub>2</sub>	0.03	0.01	0.00	0.09	0.22	0.26	b.d.l.	0.01	b.d.l.	0.08	0.38
PbO	0.22	0.31	0.00	0.15	0.39	0.19	b.d.l.	0.01	b.d.l.	b.d.l.	0.01
F	b.d.l.	b.d.l.	0.11	0.09	b.d.l.						
O = F	0.00	0.00	0.00	0.00	0.00	0.00	0.00	0.00	0.05	0.05	0.00
Total	93.85	94.91	88.56	95.76	93.32	93.31	94.64	98.03	94.86	91.71	97.81
apfu, O = 4											
Si	0.97	1.04	1.13	1.10	1.01	1.03	0.95	1.06	1.02	0.99	1.02
P	0.01	0.00	0.00	0.00	0.01	0.00	0.01	0.01	0.03	0.04	0.04
Al	0.11	0.10	0.12	0.09	0.14	0.16	0.12	0.13	0.09	0.09	0.09
Ti	0.06	0.04	0.03	0.03	0.05	0.05	n.d.	n.d.	n.d.	n.d.	n.d.
Zr	0.04	0.01	0.04	0.04	0.07	0.13	0.01	0.02	0.00	0.00	0.00
Ca	0.14	0.12	0.12	0.09	0.15	0.13	0.09	0.12	0.18	0.12	0.09
Fe	0.06	0.01	0.00	0.01	0.01	0.06	0.02	0.01	0.02	0.01	0.02
Mn	n.d.	n.d.	n.d.	n.d.	n.d.	n.d.	0.00	0.00	0.00	0.00	0.00
Sc	n.d.	n.d.	n.d.	n.d.	n.d.	n.d.	0.00	0.00	0.00	0.01	0.01
Y	0.05	0.06	0.07	0.05	0.08	0.09	0.00	0.00	0.04	0.07	0.05
La	n.d.	n.d.	n.d.	n.d.	n.d.	n.d.	0.00	0.00	0.00	0.00	0.00
Ce	0.03	0.04	0.04	0.03	0.05	0.04	0.01	0.01	0.00	0.02	0.02
Pr	n.d.	n.d.	n.d.	n.d.	n.d.	n.d.	0.00	0.00	0.00	0.00	0.00
Nd	n.d.	n.d.	0.01	n.d.	n.d.	n.d.	0.00	0.00	0.00	0.01	0.01
Sm	n.d.	n.d.	n.d.	n.d.	n.d.	n.d.	0.00	0.00	0.00	0.00	0.00
Gd	0.01	0.01	n.d.	0.00	0.01	0.01	0.00	0.00	0.00	0.01	0.01
Dy	n.d.	n.d.	n.d.	n.d.	n.d.	n.d.	0.00	0.00	0.00	0.00	0.00
Er	n.d.	n.d.	n.d.	n.d.	n.d.	n.d.	0.00	0.00	0.00	0.00	0.00
Yb	0.00	0.00	0.00	0.00	0.00	0.00	0.00	0.00	0.00	0.00	0.00
U	0.67	0.68	0.55	0.64	0.58	0.47	0.87	0.73	0.75	0.72	0.73
Th	0.00	0.00	0.00	0.00	0.00	0.00	0.00	0.00	0.00	0.00	0.00
Pb	0.00	0.00	0.00	0.00	0.00	0.00	0.00	0.00	0.00	0.00	0.00
Total	2.15	2.11	2.11	2.08	2.16	2.17	2.08	2.09	2.13	2.09	2.09

n.d.—not determined; b.d.l.—below detection limit.

#### 4.3. Brannerite

Brannerite is the most important uranium mineral in both investigated uranium deposits from the Bor pluton (Zadní Chodov and Lhota). It occurs as acicular aggregates and/or irregular grains. Larger brannerite grains are usually highly heterogeneous and on the rim are often altered to Ti-enriched brannerite and/or rutile (Figure 10). Brannerite from the Rožná uranium deposit is far less common in uranium ores. Here, brannerite was often decomposed to Ti-rich (over 90 wt % TiO<sub>2</sub>) and more complex non-stoichiometric U–Ti–Si–Zr phases during superimposed alteration processes.

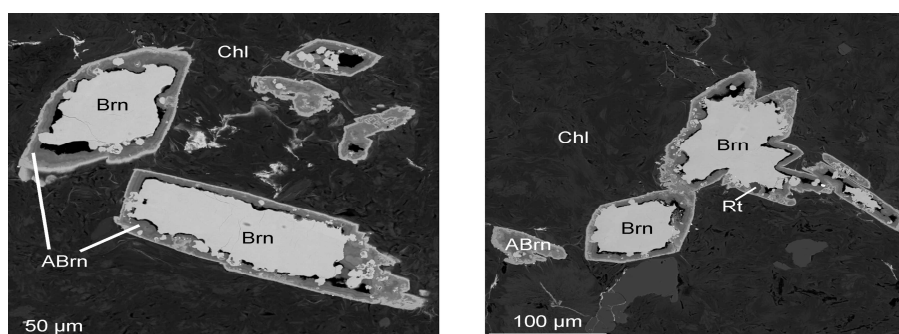


**Figure 10.** BSE images of brannerite (Brn), altered brannerite (Abrn), and rutile (Rt) enclosed in fine-grained chlorite (Chl), Zadní Chodov, taken by P. Gadas and R. Škoda.

The representative compositions of unaltered brannerite from the Rožná and Zadní Chodov uranium deposits are given in Table 3. The highly altered brannerite from the Zadní Chodov uranium deposit is depleted in U and enriched in Ti, Si, and Al. Correlations of Ti vs. U, Ca vs. U, Si vs. U, and Fe + Al vs. Ti in brannerites from Rožná and Zadní Chodov are displayed in Figure 11.

**Table 3.** Representative WDX analyses of brannerite. The apfu values are normalised to six atoms of oxygen. The total uranium determined by the microprobe was recalculated to U<sup>4+</sup> and U<sup>6+</sup> on the basis of three cations per formula unit.

Sample	1	4	13	15	28	29	31-1	33
Locality (wt %)	Rožná	Rožná	Rožná	Rožná	Zadní Chodov	Zadní Chodov	Zadní Chodov	Zadní Chodov
UO <sub>2</sub>	0.00	1.00	0.00	0.00	25.68	30.00	28.50	27.80
UO <sub>3</sub>	39.55	39.90	36.15	38.15	27.22	25.91	26.40	26.80
ThO <sub>2</sub>	n.d.	n.d.	n.d.	n.d.	0.04	0.04	0.19	0.14
TiO <sub>2</sub>	30.74	30.58	28.08	26.59	37.39	36.73	36.45	37.38
FeO	0.97	1.24	3.08	0.93	1.78	2.02	1.48	1.97
CaO	6.42	6.14	5.78	6.75	2.96	2.50	2.99	3.27
MnO	b.d.l.	b.d.l.	0.24	0.11	0.48	0.47	0.42	0.47
SiO <sub>2</sub>	11.37	12.12	13.40	14.82	0.05	0.02	0.61	0.30
ZrO <sub>2</sub>	3.24	3.23	2.46	4.82	0.29	0.08	0.19	0.33
Sc <sub>2</sub> O <sub>3</sub>	n.d.	n.d.	n.d.	n.d.	0.35	0.31	0.28	0.22
Nb <sub>2</sub> O <sub>5</sub>	n.d.	n.d.	n.d.	n.d.	0.06	0.09	0.15	0.06
Al <sub>2</sub> O <sub>3</sub>	1.15	1.63	2.48	1.77	0.01	0.00	0.29	0.03
PbO	n.d.	n.d.	n.d.	n.d.	0.01	0.02	0.05	0.00
Ce <sub>2</sub> O <sub>3</sub>	n.d.	n.d.	n.d.	n.d.	0.47	0.25	0.28	0.25
Pr <sub>2</sub> O <sub>3</sub>	n.d.	n.d.	n.d.	n.d.	0.16	0.05	0.04	0.04
Nd <sub>2</sub> O <sub>3</sub>	n.d.	n.d.	n.d.	n.d.	0.71	0.17	0.15	0.43
Sm <sub>2</sub> O <sub>3</sub>	n.d.	n.d.	n.d.	n.d.	0.27	0.14	0.16	0.21
Gd <sub>2</sub> O <sub>3</sub>	n.d.	n.d.	n.d.	n.d.	0.14	0.09	0.24	0.08
Tb <sub>2</sub> O <sub>3</sub>	n.d.	n.d.	n.d.	n.d.	0.00	0.01	0.03	0.00
Dy <sub>2</sub> O <sub>3</sub>	n.d.	n.d.	n.d.	n.d.	0.17	0.13	0.04	0.04
Er <sub>2</sub> O <sub>3</sub>	n.d.	n.d.	n.d.	n.d.	0.02	0.08	0.10	0.11
Yb <sub>2</sub> O <sub>3</sub>	n.d.	n.d.	n.d.	n.d.	0.06	0.01	0.05	0.07
Y <sub>2</sub> O <sub>3</sub>	n.d.	n.d.	n.d.	n.d.	0.51	0.44	0.40	0.41
Total	93.44	95.84	91.67	93.94	98.83	99.56	99.49	100.31
apfu, O = 6								
U <sup>4+</sup>	0.00	0.01	0.00	0.00	0.38	0.46	0.43	0.40
U <sup>6+</sup>	0.47	0.46	0.42	0.44	0.37	0.36	0.36	0.36
Ti <sup>4+</sup>	1.30	1.26	1.18	1.09	1.82	1.81	1.78	1.80
Fe <sup>2+</sup>	0.05	0.06	0.14	0.04	0.10	0.11	0.08	0.11
Ca <sup>2+</sup>	0.39	0.36	0.35	0.40	0.21	0.18	0.21	0.23
Mn <sup>2+</sup>	0.00	0.00	0.01	0.01	0.03	0.03	0.02	0.03
Si <sup>4+</sup>	0.64	0.66	0.75	0.81	0.00	0.00	0.04	0.02
Zr <sup>4+</sup>	0.09	0.09	0.07	0.13	0.01	0.00	0.01	0.01
Sc <sup>3+</sup>	n.d.	n.d.	n.d.	n.d.	0.02	0.02	0.02	0.01
Nb <sup>5+</sup>	n.d.	n.d.	n.d.	n.d.	0.00	0.00	0.00	0.00
Al <sup>3+</sup>	0.08	0.10	0.16	0.11	0.00	0.00	0.02	0.00
Ce <sup>3+</sup>	n.d.	n.d.	n.d.	n.d.	0.01	0.01	0.01	0.01
Pr <sup>3+</sup>	n.d.	n.d.	n.d.	n.d.	0.00	0.00	0.01	0.00
Nd <sup>3+</sup>	n.d.	n.d.	n.d.	n.d.	0.02	0.00	0.00	0.01
Sm <sup>3+</sup>	n.d.	n.d.	n.d.	n.d.	0.01	0.00	0.00	0.00
Gd <sup>3+</sup>	n.d.	n.d.	n.d.	n.d.	0.00	0.00	0.00	0.00
Tb <sup>3+</sup>	n.d.	n.d.	n.d.	n.d.	0.00	0.00	0.00	0.00
Dy <sup>3+</sup>	n.d.	n.d.	n.d.	n.d.	0.00	0.00	0.00	0.00
Er <sup>3+</sup>	n.d.	n.d.	n.d.	n.d.	0.00	0.00	0.00	0.00
Yb <sup>3+</sup>	n.d.	n.d.	n.d.	n.d.	0.00	0.00	0.00	0.00
Y <sup>3+</sup>	n.d.	n.d.	n.d.	n.d.	0.02	0.02	0.01	0.01
Total	3.02	3.00	3.08	3.03	3.00	3.00	3.00	3.00

n.d.—not determined; b.d.l.—below detection limit.

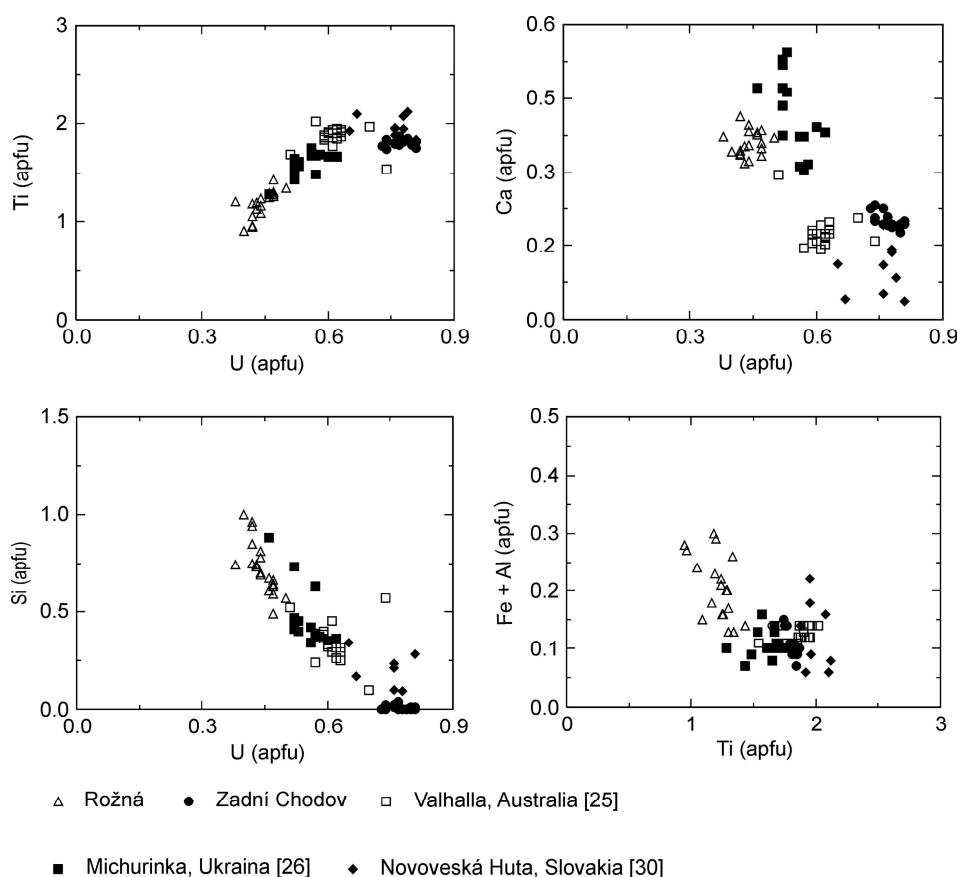


**Figure 11.** Chemical composition of brannerite and altered brannerite.

## 5. Discussion

### 5.1. Origin and Evolution of Aceites

Four to six stages of hydrothermal alteration can be distinguished on the investigated uranium deposits bound by brittle shear zones developed in high-grade metamorphic rocks and/or granites [3,6,7]. Usually pre-uranium, uranium, and post-uranium stages are distinguished. The pre-uranium stage is represented mainly by chlorite I ( $Fe/(Fe + Mg) = 0.30\text{--}0.73$ ) and albite I ( $An_{0.0\text{--}0.9}$ ), which originated by chloritisation of biotite and albitisation of original plagioclases ( $An_{20\text{--}50}$ ). The first generation of uranium minerals (uraninite, coffinite, brannerite), together with younger generations of albite and chlorite ( $Fe/(Fe + Mg) = 0.12\text{--}0.54$ ), originated during the subsequent uranium-stage [3,7].

The differences in the mineralogical composition of the rock environment of the studied uranium deposits (high-grade metamorphic rocks vs. two-mica granites, biotite granites, and biotite granodiorites) are expressed by the different composition of aceites and by distinctly more intensive tectonic movements on shear zones evolved in high-grade metamorphic rocks (Rožná, Zadní Chodov). The most significant textural features of aceites that evolved in altered granitic rocks (Okrouhlá Radouň, Lhota) is that cavities in the rock matrix composed of albite I, chlorite I, and hematite framework are filled up with younger generations of albite II, chlorite II and III, and carbonates (calcite, dolomite). However for the shear zones, which are evolved in high-grade metasediments (Rožná, Okrouhlá Radouň, Zadní Chodov), the occurrences of fine-grained chlorite I and clay minerals are characteristic. The infilling of shear zones hosted by high-grade metamorphic rocks at the Rožná, Okrouhlá Radouň, and Zadní Chodov uranium deposits also differ in composition of the assemblage of clay minerals.

The Fe-illite predominates at the Rožná ore deposit, whereas the Okrouhlá Radouň ore deposit contains mainly smectite, and in the shear zones at Zadní Chodov chlorite predominates over illite.

The uranium stage represents the Variscan uranium mineralisation event (260–280 Ma) [3,12]. The post-uranium stage is usually represented by older quartz and younger carbonate substages. During the post-uranium stage, some younger generations of uranium minerals originated (uraninite, coffinite, brannerite). The age of 158–185 Ma of uraninite and brannerite from the Okrouhlá Radouň, Lhota, and Zadní Chodov ore deposits represents the Mesozoic recrystallisation of the Variscan uranium minerals [3,6,12].

### 5.2. Sources of Metals and P-T-X Characteristics of Fluids

Uranium in the host high-grade metasediments and granitic rocks of all investigated uranium deposits is essentially hosted in monazite, and also locally (in two-mica granites at the Okrouhlá Radouň area) in xenotime [3,6,7]. In barren aceites, monazite and xenotime are usually missing. Therefore, the source of uranium may be found in the hydrothermal alteration/decomposition of uranium-bearing accessories, as is proposed for the unconformity-type uranium deposits in Canada [15]. The titanium necessary for the formation of brannerite at the Zadní Chodov and Rožná uranium deposits was probably released during chloritisation of Ti-enriched biotite and hydrothermal alteration of the Ti-rich accessories (titanite, allanite), which occur in granodiorites of the Bor pluton and in paragneisses and amphibolites of the Moldanubian Zone at the Rožná uranium deposit [3,7]. This model partly conforms with the ideas of Dill [1] who proposed hydrated Ti-oxides, which originated during pre-uranium chloritisation of biotite, as a possible source of Ti for brannerite from similar uranium deposits in Bavaria (e.g., Wäldel/Mähring).

A prominent hematitisation in the Okrouhlá Radouň, Lhota, and deeper parts of the Rožná uranium deposits indicates deep infiltration of oxidized, surface-derived fluids to the crystalline basement during the barren pre-uranium stage. The deep circulation of fluids of the pre-uranium stage gave rise to desilicified, hematitised, and albitised altered rocks (aceites).

In contrast to episyenites, which are usually products of the late magmatic alteration of granites, the aceites at the Rožná, Okrouhlá Radouň, and Zadní Chodov uranium deposits developed from metamorphic rocks. The fluids responsible for the alteration of rocks of the pre-uranium stage differ from the earlier low-salinity metamorphic fluids in their generally higher but highly variable salinities (Rožná: 7.3–21.8 wt % NaCl<sub>eq</sub>; Okrouhlá Radouň: 0–25 wt % NaCl<sub>eq</sub>). Important differences in the salinity of the pre-uranium fluids probably reflect the mixing of chemically heterogeneous basinal brines with meteoric water. The fluid inclusion data from the Rožná and Okrouhlá Radouň uranium deposits suggest low homogenisation temperatures (about 50–206 °C) during the pre-uranium stage. The available fluid inclusion and stable isotope data suggest participation of three fluid end members during alteration and mineralisation at these deposits: (i) local meteoric water; (ii) Na–Ca–Cl basinal brines or shield brines; (iii) SO<sub>4</sub>–NO<sub>3</sub>–Cl–(H)CO<sub>3</sub> playa-like fluids [3,6].

### 5.3. Behaviour of Zirconium and Yttrium in Coffinite

Zirconium and Y are typical high field strength elements (HFSE), which are generally considered immobile during hydrothermal processes [16]. Some experimental data and natural evidence, however, have demonstrated that these elements may be mobile in hydrothermal environments, especially if the fluids contained strong complexation agents such as fluoride or phosphate anions [17]. In F- and P-poor hydrothermal systems, the mobility of Y and Zr may be promoted by sulphate complexing [18]. The mobility of zirconium in aceites from the Okrouhlá Radouň uranium deposit is suggested from the occurrence of Zr-enriched coffinite developed around an altered grain of zircon (Figure 8a). Strongly altered zircon grains were also found in aceites from the Rožná uranium deposit [2].

The elevated concentrations of Zr and/or Y in coffinites are also rare worldwide. Coffinite enriched in Zr and Y associated with U-Zr-silicates has also been found in the natural fission reactor of the Oklo uranium deposit, Gabon [19]. A hydrothermal mineral association formed by Zr-rich coffinites

was described from a fault-related uranium occurrence in Outsdale, Scotland [20]. Yttrium-enriched coffinites have been described from the Grants uranium region in New Mexico, USA [21], and the Witwatersrand uranium deposit in South Africa [22]. Coffinite enriched in Zr and Y and associated with U-Zr-silicates has also been found in uranium deposits from the Mount Isa region of Queensland, Australia [23]. In all these cases, the source of Y and Zr is thought to be in xenotime and zircon occurring in the wall rocks.

#### 5.4. Occurrence and Chemical Composition of Brannerite

Brannerite occurs as a significant uranium mineral in high-temperature Na-metasomatic uranium deposits in the Central Ukrainian province [24] and medium-temperature Na-metasomatic uranium deposits in Guyana and Australia [25,26]. For all of these uranium deposits, the Na-Ca alteration is coupled with basinal and magmatic fluids and the occurrence of sodic amphiboles and pyroxenes are characteristic. In contrast to these uranium deposits, the alteration zones of the studied uranium deposits (Rožná, Okrouhlá Radouň, Zadní Chodov, Lhota) originated during low-temperature Na-alteration, giving rise to albite, chlorite, and hematite as the most important hydrothermal minerals.

The chemical composition of brannerite is nominally  $UTi_2O_6$ . However, brannerite is commonly deficient in uranium and has an excess of titanium relative to the ideal formula [27,28]. Analysed brannerites from the Zadní Chodov uranium deposit display high Ti concentrations, distinctly higher than brannerites from the Na-metasomatic uranium deposits (Michurinka, Central Ukraine; Valhalla, Australia) [24,26]. However, brannerites from the Rožná uranium deposits are depleted in Ti (Figure 11). Furthermore, in brannerite U may be replaced by Ca, Th, Y, and REE, while Si, Al, and Fe can replace Ti as a result of oxidation and partial hydration [29]. The most likely substitution of U by Ca is  $Ca^{2+} + U^{6+} \rightarrow 2U^{4+}$  [30]. Brannerites from the Rožná uranium deposit have a comparably high content of Ca whereas unaltered brannerites from the Zadní Chodov ore deposit are depleted in Ca, when compared with brannerites from Ukraine (Figure 11). All these brannerites are enriched in Ca in comparison with brannerites from the Novoveská Huta uranium deposit, which is related to the Permian acid volcanism. The presence of Pb in the brannerite structure is mainly due to the decay of U. The unaltered brannerites from the Zadní Chodov uranium deposit are depleted in Si and Al in comparison with the brannerites from Australia (Mt Isa, Valhalla), Guyana, Ukraine [24–26,31], and Novoveská Huta [31]. However, brannerites from the Rožná ore deposit have relatively high Si and Al contents (Figure 11). Unaltered brannerites have usually calculated  $U^{4+}/(U^{4+} + U^{6+})$  ratios in the range of 0.35 to 0.95. Altered brannerites from the Zadní Chodov and Rožná uranium deposits display very low  $U^{4+}/(U^{4+} + U^{6+})$  ratios (0–0.26). Lower  $U^{4+}/(U^{4+} + U^{6+})$  ratios could be associated with brannerite oxidation [30] (Figure 10). Similar altered brannerites with low  $U^{4+}/(U^{4+} + U^{6+}) = 0–0.24$  ratios were found in Crocker's Well (Australia) and San Bernardino County, California [28].

## 6. Conclusions

Disseminated coffinite-uraninite and coffinite-brannerite mineralisation occurs in shear zones of the Rožná, Okrouhlá Radouň, Zadní Chodov, and Lhota uranium deposits which are found in high-grade metamorphic rocks of the Moldanubian Zone and in granitic rocks of the Bor pluton. The analysed uraninite from the Rožná ore deposit is strongly coffinitised and displays very high  $SiO_2$  contents (6.3–13.0 wt %). Coffinites from the Rožná and Okrouhlá Radouň uranium deposits are enriched in  $Y_2O_3$  (up to 3.4 wt %) and  $ZrO_2$  (up to 13.8 wt %). Brannerite is present in unaltered and altered grains with variable  $U^{4+}/(U^{4+} + U^{6+})$  ratios. The unaltered brannerites have  $U^{4+}/(U^{4+} + U^{6+})$  ratios between 0.38 and 0.65, whereas the altered brannerites display these ratios distinctly lower (0–0.26).

The source of uranium may be found in the hydrothermal decomposition of uranium-bearing accessories occurring in host high-grade metasedimentary and granitic rocks (monazite, xenotime). The large-scale hydrothermal alteration of host rocks, as well the observed mobility of Y, Zr, and Ti

indicates a significant fault-related influx of oxidized basinal fluids into the basement rocks of the Moldanubian Zone during the formation of acetics and associated uranium mineralisation.

**Acknowledgments:** The research for this paper was carried out thanks to the support of the long-term conceptual development research organisation RVO 67985891. Part of analytical costs was covered by project IGA UP PrF/2015/014. P. Gadas and R. Škoda from the Masaryk University, Brno are thanked for their assistance during the microbe work. We wish to thank the three anonymous reviewers for their perceptive reviews of the manuscript, valuable comments, and recommendations.

**Author Contributions:** Miloš René contributed the majority of the analysed samples and wrote the paper, Zdeněk Dolníček contributed the uraninite sample from the Rožná uranium deposit and analysed the uraninite from the Okrouhlá Radouň ore deposit and brannerite from the Zadní Chodov uranium deposit.

**Conflicts of Interest:** The authors declare no conflict of interest.

## References

- Dill, H. Lagerstättengenetische Untersuchungen in Bereich der Uranerz-Struktur Wäldel/Mähring (NE-Bayern). *Geol. Rundsch.* **1983**, *72*, 329–352. (In German). [[CrossRef](#)]
- René, M. Anomalous rare earth element, yttrium and zirconium mobility associated with uranium mineralization. *Terra Nova* **2008**, *20*, 52–58. [[CrossRef](#)]
- Křibek, B.; Žák, K.; Dobeš, P.; Leichmann, J.; Pudilová, M.; René, M.; Scharm, B.; Scharmová, M.; Hájek, A.; Holeczy, D.; et al. The Rožná uranium deposit (Bohemian Massif, Czech Republic): Shear zone-hosted, late Variscan and post-Variscan hydrothermal mineralization. *Miner. Deposita* **2009**, *44*, 99–128. [[CrossRef](#)]
- René, M. Uranium hydrothermal deposits. In *Uranium: Characteristics, Occurrence and Human Exposure*; Vasiliev, A.Y., Sidorov, M., Eds.; Nova Science Publishers Inc.: New York, NY, USA, 2012; pp. 211–244.
- Uranium 2014: Resources, Production and Demand*; OECD Nuclear Energy Agency: Paris, France, 2014; p. 508.
- Dolníček, Z.; René, M.; Hermannová, S.; Prochaska, W. Origin of the Okrouhlá Radouň episyenite-hosted uranium deposit, Bohemian Massif, Czech Republic: Fluid inclusion and stable isotope constraints. *Miner. Deposita* **2014**, *49*, 409–425. [[CrossRef](#)]
- René, M. Alteration of granitoids and crystalline rocks and uranium mineralisation in the Bor pluton area, Bohemian Massif, Czech Republic. *Ore Geol. Rev.* **2017**, *81*, 188–200. [[CrossRef](#)]
- Fettes, D.; Desmons, J. (Eds.) *Metamorphic Rocks: A Classification and Glossary of Terms: Recommendations of the International Union of Geological Sciences. Subcommission on the Systematics of Metamorphic Rocks*; Cambridge University Press: Cambridge, UK, 2007; p. 244.
- Cathelineau, M. The hydrothermal alkali metasomatism effects on granitic rocks: Quartz dissolution and related subsolidus changes. *J. Petrol.* **1986**, *27*, 945–965. [[CrossRef](#)]
- Kafka, J. (Ed.) *Czech Ore and Uranium Mining Industry*; Anagram: Ostrava, Czech Republic, 2003.
- Verner, K.; Žák, J.; Šrámek, J.; Paclíková, J.; Zavřelová, A.; Machek, M.; Finger, F.; Johnson, K. Formation of elongated granite–migmatite domes as isostatic accommodation structures in collisional orogens. *J. Geodyn.* **2014**, *73*, 100–117. [[CrossRef](#)]
- Ordynec, G.E.; Komínek, J.; Anderson, E.B.; Milovanov, I.A.; Nikolsky, A.L.; Romanidis, K. Alters of the uranium mineralisation of deposits at the West-Bohemian ore district. *Geol. Hydrometalurg. Uranu* **1987**, *11*, 23–64.
- Dörr, W.; Zulauf, G.; Fiala, J.; Schastok, J.; Scheuven, D.; Wulf, S.; Vejnar, Z.; Ahrendt, H.; Wemmer, K. Dating of collapse related plutons along the West- and Central Bohemian shear zones (European Variscides). *Terra Nostra* **1997**, *97*, 31–34.
- Pouchou, J.J.; Pichoir, F. “PAP” ( $\varphi$ - $\rho$ -Z) procedure for improved quantitative microanalysis. In *Microbeam Analysis*; Armstrong, J.T., Ed.; San Francisco Press: San Francisco, CA, USA, 1985; pp. 104–106.
- Hecht, L.; Cuney, M. Hydrothermal alteration of monazite in the Precambrian crystalline basement of the Athabasca Basin (Saskatchewan, Canada): Implications for the formation of unconformity-related uranium deposits. *Miner. Deposita* **2000**, *35*, 791–795. [[CrossRef](#)]
- Bau, M. Controls on the fractionation of isovalent trace elements in magmatic and aqueous systems: evidence from Y/Ho, Zr/Hf, and lanthanide tetrad effect. *Contrib. Mineral. Petrol.* **1996**, *123*, 323–333. [[CrossRef](#)]
- Giére, R. Transport and deposition of REE in H<sub>2</sub>S-rich fluids: Evidence from accessory mineral assemblages. *Chem. Geol.* **1993**, *110*, 251–268. [[CrossRef](#)]

18. Rubin, J.N.; Henry, C.D.; Price, J.G. The mobility of zirconium and other immobile elements during hydrothermal alteration. *Chem. Geol.* **1993**, *110*, 100–117. [[CrossRef](#)]
19. Jensen, K.A.; Ewing, R.C. The Okélobondo natural fission reactor, southeast Gabon: Geology, mineralogy and retardation of nuclear-reaction products. *Geol. Soc. Am. Bull.* **2001**, *113*, 32–62. [[CrossRef](#)]
20. Pointer, V.M.; Asworth, J.R.; Simpson, P.R. Genesis of coffinite and the U-Ti association in lower Old Red sandstone sediments, Ousdale, Caithness, Scotland. *Miner. Deposita* **1989**, *24*, 117–123. [[CrossRef](#)]
21. Hansley, P.L.; Fitzpatrick, J.J. Compositional and crystallographic data on REE-bearing coffinite from the Grants uranium region, northwestern New Mexico. *Am. Mineral.* **1989**, *74*, 263–279.
22. Smits, G. (U, Th)-bearing silicates in reefs of the Witwatersrand, South Africa. *Can. Mineral.* **1989**, *27*, 643–655.
23. Wilde, A.; Otto, A.; Jory, J.; MacRae, C.; Pownceby, M.; Wilson, N.; Torpy, A. Geology and Mineralogy Of Uranium Deposits from Mount Isa, Australia: Implications for Albitite Uranium Deposit Models. *Minerals* **2013**, *3*, 258–283. [[CrossRef](#)]
24. Cuney, M.; Emetz, A.; Mercadier, J.; Mykchaylov, V.; Shunko, V.; Yuslenko, A. Uranium deposits associated with Na-metasomatism from Central Ukraine: A review of some of the major deposits and genetic constraints. *Ore Geol. Rev.* **2012**, *44*, 82–106. [[CrossRef](#)]
25. Alexandre, P. Mineralogy and geochemistry of the sodium metasomatism-related uranium occurrence of Aricheng South, Guyana. *Miner. Deposita* **2010**, *45*, 351–367. [[CrossRef](#)]
26. Polito, P.A.; Kyser, T.K.; Stanley, C. The Proterozoic, albitite-hosted, Valhalla uranium deposit, Queensland, Australia: A description of the alteration assemblage associated with uranium mineralisation in diamond drill hole V39. *Miner. Deposita* **2009**, *44*, 11–40. [[CrossRef](#)]
27. Ferris, C.S.; Ruud, C.O. *Brannerite: Its Occurrences and Recognition by Microprobe*; Colorado School of Mines: Golden, CO, USA, 1971.
28. Kaiman, S. *Composition of Elliot Lake Brannerite*; Mines Branch Report EMT 73-14; Department of Energy, Mines and Resources: Ottawa, ON, Canada, 1973.
29. Smith, D.K., Jr. Uranium mineralogy. In *Uranium Geochemistry, Mineralogy, Geology, Exploration and Resources*; de Vivo, B., Ippolito, F., Capaldi, G., Simpson, P.R., Eds.; The Institution of Mining and Metallurgy: London, UK, 1984; pp. 43–88.
30. Lumpkin, G.R.; Leung, S.H.F.; Ferenczy, J. Chemistry, microstructure, and alpha decay damage of natural brannerite. *Chem. Geol.* **2012**, *291*, 55–68. [[CrossRef](#)]
31. Rojkovič, I.; Boronichin, V.A. U-Ti minerals at the deposit Novoveská Huta (Slovenské Rudohorie Mts.). *Geol. Carpath.* **1984**, *33*, 321–330.



© 2017 by the authors. Licensee MDPI, Basel, Switzerland. This article is an open access article distributed under the terms and conditions of the Creative Commons Attribution (CC BY) license (<http://creativecommons.org/licenses/by/4.0/>).